Downloaded from http://rsta.royalsocietypublishing.org/ on October 21, 2018

PHILOSOPHICAL TRANSACTIONS OF THE ROYAL SOCIETY A

Phil. Trans. R. Soc. A (2010) **368**, 1663–1679
doi:10.1098/rsta.2010.0007

Review

Small Atwood number Rayleigh–Taylor experiments

By Malcolm J. Andrews[1] and Stuart B. Dalziel[2,*]

[1]*Los Alamos National Laboratory, Los Alamos, NM 87545, USA*
[2]*Department of Applied Mathematics and Theoretical Physics, University of Cambridge, Wilberforce Road, Cambridge CB3 0WA, UK*

Consideration is given to small Atwood number (non-dimensional density difference) experiments to investigate mixing driven by Rayleigh–Taylor (R–T) instability. The past 20 years have seen the development of novel experiments to investigate R–T mixing and, simultaneously, the advent of high-fidelity diagnostics. Indeed, the developments of experiments and diagnostics have gone hand in hand, and as a result modern R–T experiments rival the capabilities and research scope of shear-driven mixing experiments. Thus, research into the small Atwood number limit has made significant progress over the past 20 years, and has offered important insights into natural mixing processes as well as the general R–T problem. This review of small Atwood number experiments serves as an opportunity to discuss progress, and also to provoke thoughts about future high Atwood number designs and difficulties.

Keywords: Rayleigh–Taylor instability; small Atwood number; turbulent mixing; experiments

1. Introduction

The Rayleigh–Taylor (R–T) instability occurs when a high-density (ρ_1) fluid is placed over a lower-density (ρ_2) fluid in a gravitational field. When the density interface is disturbed away from horizontal, the hydrostatic pressure acts to drive the heavier fluid into the lighter one, with the disturbance amplitude initially growing exponentially, but shortly afterwards saturating and forming a characteristic mushroom shape, at least for some time. Eventually, either other wavelengths become important and accelerate the development of the instability, or mixing and dilution of the density contrast will lead to a deceleration. Just such a mechanism has occurred to the cirrus clouds shown in figure 1, where the characteristic mushroom shapes of R–T instabilities form a beautiful structure along the lower edge of the cloud. Such naturally occurring R–T instabilities are quite common (e.g. in oceans, supernovae and oil-trapping salt domes), but are hard to record because of their transient nature and fast (with the exception of salt domes) transition to mixing and turbulence. R–T instability also plays an

*Author for correspondence (s.dalziel@damtp.cam.ac.uk).

One contribution of 13 to a Theme Issue ‘Turbulent mixing and beyond’.

 This journal is © 2010 The Royal Society

Downloaded from http://rsta.royalsocietypublishing.org/ on October 21, 2018

Figure 1. R–T cirrus clouds. (Photograph courtesy of David Jewitt, University of California at Los Angeles.)

important role in the mixing that results from other natural mixing processes where density surfaces are overturned, e.g. Kelvin–Helmholtz instability and breaking internal gravity waves (Turner 1973). Indeed, not only is the mixing efficiency of R–T higher than that of any other known mechanism, but it has been suggested as an explanation for the much lower mixing efficiencies due to shear or mechanical agitation (Dalziel *et al.* 2008).

This review describes recent (over the past 20 years) experiments that have sought to better understand the development of small Atwood number ($A_t \equiv (\rho_1 - \rho_2)/(\rho_1 + \rho_2) < 0.1$) R–T (buoyancy-driven) mixing. The discussion is restricted to incompressible experiments (the authors know of no compressible experiments at small Atwood number). There are few small Atwood number experiments; so this review also seeks to explain connections to high Atwood number experiments, and more generally discusses the difficulties met when trying to perform/design R–T experiments.

Next, we present a brief introduction to the R–T instability, and the development of R–T driven mixing. We focus on basic results, relevant to the small Atwood number experiments of concern in this review, and refer the reader to the extensive set of papers published in the proceedings of the 2007 Trieste conference 'Turbulent Mixing and Beyond' (see Abarzhi *et al.* 2008).

Youngs (1984) described the development of an R–T mixing region as a three-step process (somewhat paraphrased):

(1) Initially an exponential growth of infinitesimal perturbations that correspond to linear stability analysis.
(2) At amplitudes of about one-half of the wavelength, the instability saturates and longer wavelengths (that have yet to reach saturation) take over. Emmons *et al.* (1960) coined the term 'bubble competition' to describe this regime.

Downloaded from http://rsta.royalsocietypublishing.org/ on October 21, 2018

(3) Eventually, through nonlinear mode interaction and successive wavelength saturation, a self-similar R–T mixing layer is formed with a scale similarity as gt^2.

The past 20 years have seen these steps being refined, but essentially the process given by Youngs has stood the test of time. In particular, the criterion mentioned in step (2) may be as low as one-tenth of the wavelength, and it has recently been suggested (Ramaprabhu *et al.* 2006) that there is a re-acceleration of a single perturbation to another higher saturated amplitude growth rate. For step (3), the implication was that at self-similarity the mixing width grows independently of the initial conditions, and that the self-similarity is unique. Both these assumptions have been challenged in the past 10 years, such that the initial conditions for R–T mixing development have been recognized as significant (Dalziel *et al.* 1999; Mueschke *et al.* 2006). However, it is an outstanding question whether at a very late time (a somewhat vague terminology) there is only one self-similarity, in which self-interaction, via mode coupling (rather than bubble competition), is the mechanism responsible for the continued growth of the dominant horizontal as well as vertical length scales. It has also been recognized that during the development of R–T mixing there may be more than one self-similarity; in fact, there may be multiple families of similarities that depend on the initial conditions or physical parameters such as surface tension, viscosity or geometric constraints (Abarzhi *et al.* 2008; Dimonte 2008).

The three steps outlined above have corresponding formulae, which are included here as part of the review, for pure two-fluid R–T mixing (i.e. immiscible fluids; the effects of miscibility are discussed later). The exponential growth described in step (1) is captured by linear stability analysis (Drazin & Reid 1981) for a plane wavelength λ (where the wavenumber is given by $k = 2\pi/\lambda$), which gives the exponential growth rate s as

$$s = \pm\left\{kg\frac{(\rho_1 - \rho_2)}{(\rho_1 + \rho_2)}\right\}^{1/2} = \pm\{kgA_t\}^{1/2}, \tag{1.1}$$

where g is the acceleration due to gravity, which (with more generality) forms a driving hydrostatic pressure gradient. If stabilizing effects of surface tension γ are added, the growth rate changes to

$$s_\gamma = \pm\left\{\frac{k^2}{(\rho_1 + \rho_2)}\left[\frac{g(\rho_1 - \rho_2)}{k} - k\gamma\right]\right\}^{1/2}, \tag{1.2}$$

with a 'cut-off' wavelength λ_c (i.e. all wavelengths above are unstable, and those below—as s_γ becomes imaginary—are stable) given by

$$\lambda_c = \frac{2\pi}{k} = 2\pi\left\{\frac{\gamma}{g\,(\rho_1 - \rho_2)}\right\}^{1/2}. \tag{1.3}$$

The 'most unstable' wavelength λ_m that grows fastest is

$$\lambda_m = \lambda_c\sqrt{3}. \tag{1.4}$$

Downloaded from http://rsta.royalsocietypublishing.org/ on October 21, 2018

Youngs (1984) reports simplified formulae for the most unstable wavelength and growth rate when viscosity is incorporated, namely

$$\lambda_\nu \approx 4\pi \left\{ \frac{\nu^2}{g} \frac{\rho_1 + \rho_2}{\rho_1 - \rho_2} \right\}^{1/3} \quad \text{and} \quad s_\nu = \left\{ \frac{\pi g}{\lambda_\mathrm{m}} \left(\frac{\rho_1 - \rho_2}{\rho_1 + \rho_2} \right) \right\}^{1/2}, \tag{1.5}$$

where ν is the kinematic viscosity. Many approaches have been proposed for the saturation velocity (see Abarzhi *et al.* 2003; Ramaprabhu & Dimonte 2005). In particular, the model by Goncharov (2002) predicts the saturation velocity of a two-dimensional disturbance (bubble) with wavenumber k, which is given by

$$V_{b,\infty}^{\mathrm{2D}} = 1.025 \sqrt{\frac{2A_t}{1 + A_t} \frac{g}{3k}}, \tag{1.6}$$

and for a three-dimensional disturbance by

$$V_{b,\infty}^{\mathrm{3D}} = 1.02 \sqrt{\frac{2A_t}{1 + A_t} \frac{g}{k}}. \tag{1.7}$$

At high Atwood number, these formulae reduce to those of Layzer (1955).

At late time, the self-similarity half-width h of a small Atwood number R–T mixing region is described by

$$h = \alpha A_t g t^2. \tag{1.8}$$

This last formula defines the 'α' growth-rate parameter that has been the centre of R–T research over the past 20 years. Recent work from Ristorcelli & Clark (2004) has shown a more general second-order polynomial similarity that is dominated by equation (1.8) at late time.

At small density differences, $A_t < 0.1$, up-welling ('bubble') and down-welling ('spike') disturbances form a symmetrical mixing region that expands away from the initial position of the density interface. The assignment of $A_t < 0.1$ is somewhat arbitrary, and is based on the reviewers' experience rather than on any extensive reported study; indeed, asymmetries in the penetration of rising bubbles and falling spikes are not readily apparent until $A_t > 0.5$. Figure 2 shows a planar laser-induced fluorescence (PLIF) photograph taken in the R–T water tunnel experiment at Texas A&M University (Kraft *et al.* 2005) (see §2*d*). The laser sheet is 1 mm thick and the fluorescing fluid contains rhodamine dye. The top fluid in figure 2 is cold water (20°C), overlaying warm water (25°C). The characteristic R–T mushroom shapes can be observed with little apparent diffusion, but the diffusivity of heat (temperature) with a Prandtl number (Pr, ratio of momentum and heat diffusivities) of approximately 7 is much higher than the mass diffusivity of the dye with a Schmidt number (Sc, ratio of momentum and dye diffusivities) of approximately 1000, illustrating one of the difficulties of observing R–T structures and their development. More details of the experiment and results are given later in §2*d*. Figure 3 serves to define the typical nomenclature used in the R–T research field. In particular, h_1 is the penetration distance, from the initial position of the density interface, of the light bubble, and h_2 is the corresponding penetration of the heavy spike. For the present small Atwood number case, the bubble and spike penetrations are

Downloaded from http://rsta.royalsocietypublishing.org/ on October 21, 2018

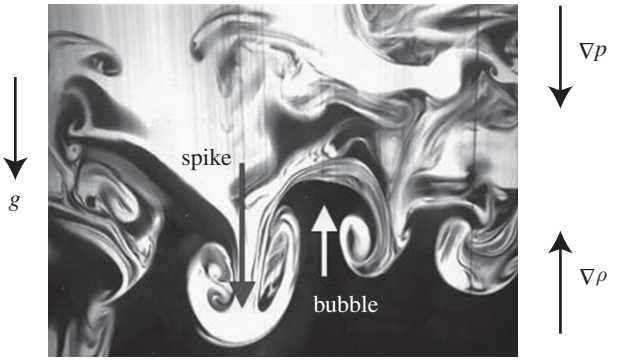

Figure 2. Characteristic shapes of R–T mixing at small Atwood number.

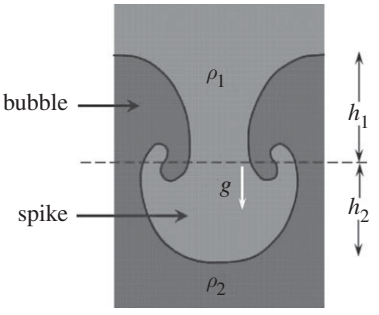

Figure 3. R–T nomenclature and parameter definitions.

very nearly the same (symmetric). As the Atwood number increases, the spike penetration is greater than that of the bubble owing to a narrowing of the spike, and a consequent reduction of drag on the head of the spike. It is typical in these small Atwood number, incompressible, experiments to invoke the Boussinesq assumption for buoyancy-driven flows (quite different from the Boussinesq model in turbulence), which states that density difference effects need only be accounted for in the gravitational terms, and density may be taken as a constant elsewhere in the equations. At small Atwood number ($A_t \ll 1$) the Boussinesq approximation is valid; however, at large A_t (approx. 1) it implies a symmetry to the flow that is contrary to the familiar bubbles and spikes of water falling out of a glass. So we (somewhat arbitrarily) assign the Boussinesq assumption as valid only for $A_t < 0.1$.

2. Small Atwood number experiments

(*a*) *Background*

The first 'modern' R–T mixing experiments were those of the well-known 'rocket rig' (RR) of Read & Youngs (1983), Read (1984), Burrows *et al.* (1984) and Smeeton & Youngs (1987). In short, the experiments involved acceleration

Downloaded from http://rsta.royalsocietypublishing.org/ on October 21, 2018

downwards of two-dimensional or three-dimensional boxes filled with light fluid over heavy fluid. The downward acceleration (up to 50 times gravity) set up an unstable R–T interface that then drove the development of R–T mixing. The experiment only considered high Atwood numbers (more than 0.2), and only a few experiments were done with miscible fluids. This RR experiment is now considered a classic by most in the R–T research field, and inspired the linear electric motor (LEM) experiment of Dimonte & Schneider (1996). One problem with the RR experiments, which used miscible fluids, is that the interface in a miscible experiment will smear due to diffusion, and this in turn can lead to a delay in the development of the mixing (due to a reduction in the driving buoyancy gradient). The third report of Smeeton & Youngs (1988) makes this point well, and, based on the theory by LeLevier *et al.* (1955), estimates the time delay as $t_{\mathrm{delay}} = 10\tau_{\mathrm{m}}$, where τ_{m} is the e-folding time for the maximum growth rate perturbation associated with a density variation that drops from ρ_1 to ρ_2 over a distance Δ under an imposed acceleration $g_{\mathrm{acc}} = g_{\mathrm{box}} - g_{\mathrm{grav}}$ (and is a modified version of equation (1.1) that would still be applicable if $\lambda \gg \Delta$, typical of the miscible experiments reviewed in §2*b–d*):

$$\tau_{\mathrm{m}} = \left(\frac{\Delta}{2g_{\mathrm{acc}}} \frac{\rho_1 + \rho_2}{\rho_1 - \rho_2} \right)^{1/2}. \tag{2.1}$$

So the distance S moved by the accelerating box over this delay period is

$$S = \frac{1}{2} g_{\mathrm{acc}} (10\tau_{\mathrm{m}})^2 = \frac{100}{4A_t} \Delta. \tag{2.2}$$

The implications of this formula are best understood by substituting some values. In particular, if the Atwood number is 0.1 and $\Delta = 5$ mm, then the distance moved is approximately 1.25 m, much of the length of the apparatus. Smaller Atwood numbers result in longer delay distances. Higher Atwood numbers shorten the delay and its associated distance, providing a longer development period for the R–T mixing. An alternative is to avoid miscible fluids and use immiscible ones, as done in the RR and LEM experiments.

Even immiscible RR and LEM experiments may be problematical at small Atwood number. In particular, using the mixing width formula of equation (1.8) with a measured α of 0.07, a mixing width of half the box height, $H/2$ (i.e. the box is filled with mixing), and taking $g_{\mathrm{acc}} \gg g_{\mathrm{grav}}$, the time and hence distance moved by the box, S, is $S = H/(4\alpha A_t)$. If A_t is small (less than 0.01), the distance moved by the box to this late-time (full box) mixed state is $S > 300H$, and so the distance required for the box to accelerate becomes a potential difficulty (if H is only 10 cm, the required distance is greater than 30 m).

One consequence of these considerations is the introduction of stationary R–T experiments that can explore small Atwood numbers—i.e. experiments that employ gravity and various innovative methods to place the heavy fluid above the light one. In this regard, to date, there have been three such experiments, which are described in the following sections. Each experiment uses miscible fluids, and explores R–T turbulent mixing; the effect of miscibility is to mitigate the instability growth rate at wavelengths of approximately Δ, as per the most unstable wavelength of equation (2.1). Perhaps the most interesting effect of miscibility is the effect of the Schmidt number (Sc) or equivalently

Downloaded from http://rsta.royalsocietypublishing.org/ on October 21, 2018

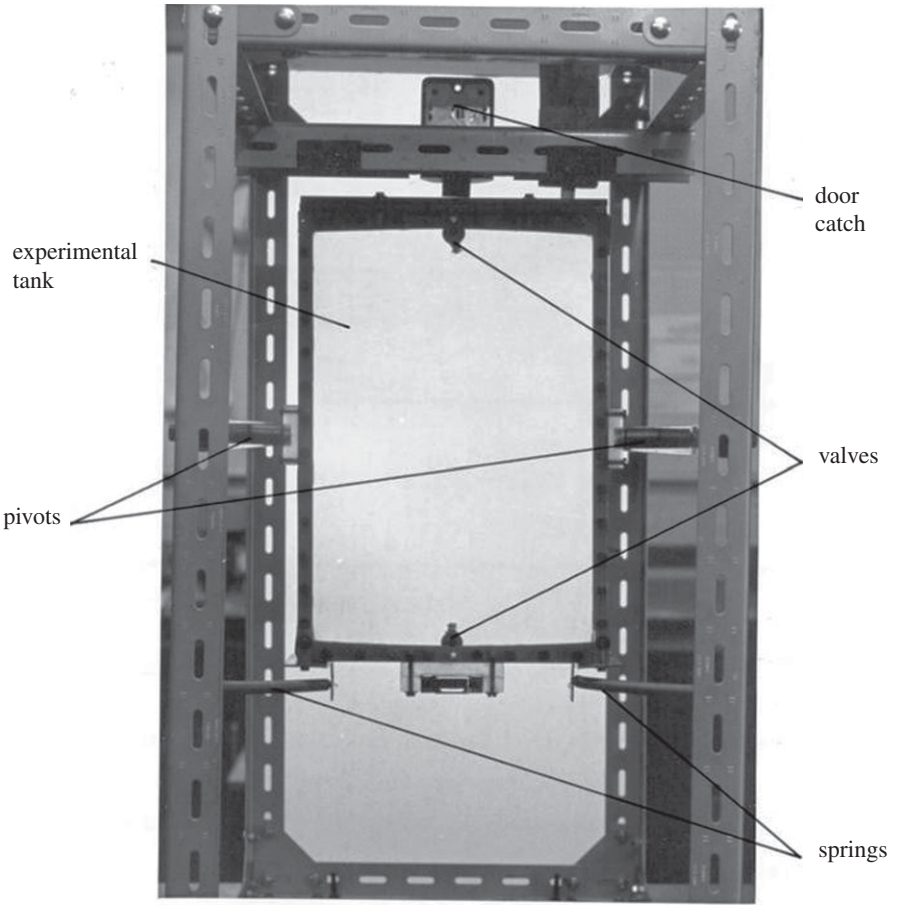

Figure 4. The overturning tank of Andrews & Spalding (1990).

the Prandtl number (Pr) on molecular mixing, as discussed in §2*e*, wherein brine/water R–T mixing has Sc approximately 700 and hot/cold water has Pr approximately 7.

(*b*) *The overturning tank*

Figure 4 shows a photograph of the overturning tank (OT) R–T experiment performed by Andrews (1986) during his PhD thesis, with details available in Andrews & Spalding (1990). The apparatus was constructed after several failed attempts at producing a quantitative and/or useful R–T experimental facility, and comprises a narrow tank (0.5 cm), with a height of 36 cm and breadth of 25 cm. The tank pivots around its centre, as shown in figure 4, and when released is spun 180° by springs and caught at the top by a door catch, thereby placing heavy brine solution ($\rho_1 = 1.10\,\mathrm{g\,cm^{-3}}$) above fresh water ($\rho_2 = 1.0\,\mathrm{g\,cm^{-3}}$). As this photograph shows, in addition to running the experiment with an initially horizontal interface, the rig could also be tilted (i.e. a wedge placed on one side) to

Downloaded from http://rsta.royalsocietypublishing.org/ on October 21, 2018

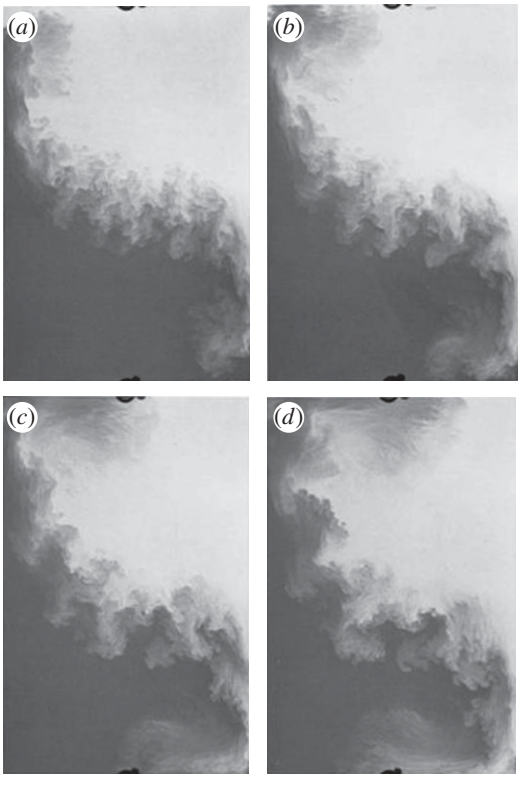

Figure 5. Tilted-rig experiments from the overturning tank; initial tilt angle of 55′ and $A_t = 0.048$. Times: (*a*) $t = 2.0$ s, (*b*) $t = 2.2$ s, (*c*) $t = 2.4$ s and (*d*) $t = 2.6$ s.

generate an initial long wavelength (half a sawtooth). The photographs in figure 5 show the R–T flow development of a tilted experiment, and even with such a small tilted angle of 0.9°, a distinct two-dimensional overturning flow develops. Closer inspection of figure 5 reveals that the centre of the mixing is developing as if it were a flat interface (clear R–T bubbles and spikes can be seen), and the width of this central region gave a measure of α of 0.04. In retrospect, this low experimental value of 0.04 was probably due to the narrow (0.5 cm) flow domain, forcing the flow to be predominantly two dimensional and perhaps being significantly affected by the front and back walls. At later time, the initial tilt gives rise to an overturning motion that starts with jets appearing at the sides of the box. These jets are attributed to the rapid growth of high-wavenumber components in the initial, half-sawtooth, tilted interface. As the overturning motion develops, the longer-wavelength initial perturbations serve to rotate the central mixing region and stretch it out, causing the central mix to thin. Such two-dimensional R–T experiments are growing in importance, as they represent new challenges for the development of multi-dimensional turbulence models of R–T mixing.

The OT overcame the issue of mixing development time at small Atwood number by inverting the position of the different density fluids, and holding the configuration steady until mixing was complete. With the box being stationary,

Downloaded from http://rsta.royalsocietypublishing.org/ on October 21, 2018

diagnostic and visualization hardware could remain stationary, and high time resolution could be obtained. However, like all R–T experiments, the OT experiment suffered from several difficulties, which included the following:

— The narrow gap between the front and back plates, necessary to prevent significant sloping during the overturn, forced the R–T flow to be two dimensional.
— The transient nature of the experiment meant that, to obtain reasonable statistics, the same experiment needed to be run multiple times (perhaps as many as 50 times) and this was not feasible at the time.
— The finite time to overturn the box gave a tilt to the interface across the narrow gap associated with the inviscid response of a density-stratified fluid under gravity, which in turn produced an initial mixing region that was quite wide (about 1 cm) and hid the early-time development of R–T mixing.
— Catching the box caused the rig to shake and introduced small perturbations, and in these experiments these were determined not to be significant (i.e. the vibrations generated wavenumbers that are higher than the most unstable and were not observed).
— Trying to perform high Atwood number experiments would have been extremely difficult, as the box would have needed to be spun at much higher speeds, and then caught without introducing unknown initial conditions.

Subsequently, OTs have been used by Voropayev *et al.* (1993) to explore R–T in a linearly stratified fluid, and by Dalziel *et al.* (2008) for R–T mixing in a high-aspect-ratio geometry, in which the buoyancy-driven three-dimensional turbulence leads to essentially one-dimensional large-scale dynamics.

(*c*) *The sliding barrier Rayleigh–Taylor experiment*

The sliding barrier (SB) experiment was developed in Cambridge University to provide low Atwood number results in a three-dimensional domain. In its first incarnation, introduced by Linden & Redondo (1991), a simple metal barrier was used to divide a cuboidal tank into two equal volumes. Fresh water beneath the barrier was separated from salt water above the barrier until the barrier was removed by sliding it through a slot at one end of the tank. The two most significant drawbacks of this approach are the finite time required to withdraw the barrier and the perturbation its removal induces. Viscous boundary layers form on the upper and lower surfaces of the barrier as it is withdrawn, leaving behind a wake with a well-defined wavelength (here about one-fifth of the length of the tank) that imposes a strong initial two-dimensional perturbation. Moreover, the viscous boundary layers are stripped from the barrier as it passes through the end wall, generating strong vortices propagating vertically away from the barrier. Despite the two-dimensional influence of the barrier, the flow rapidly develops a three-dimensional character and appears to approach a $\alpha A_t g t^2$ growth, with Linden & Redondo (1991) reporting a value of $\alpha = 0.07 \pm 0.01$, although in later work (Linden *et al.* 1994) they revised this to 0.044 ± 0.005 after introducing a virtual time origin to account for the long-wave disturbance. This rig was also used to explore, for the first time experimentally, the structure of the mixed region and quantify the degree of molecular mixing that occurred.

Downloaded from http://rsta.royalsocietypublishing.org/ on October 21, 2018

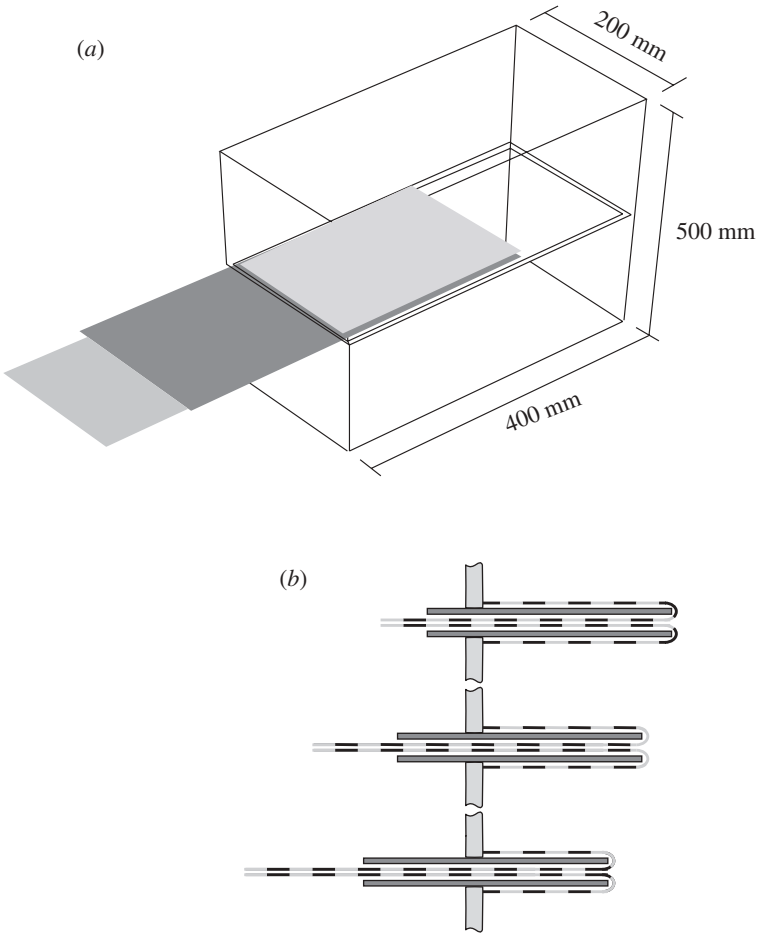

Figure 6. Composite sliding barrier tank. (*a*) Light grey shading represents nylon fabric wrapped around the dark grey metal plates. (*b*) Illustration of process by which fabric (dashed) is removed through the gap between the plates.

In an effort to eliminate the viscous boundary layers on the barrier, Dalziel (1993) introduced a modified barrier comprising a pair of horizontal plates each wrapped in nylon fabric (figure 6). The upper piece of nylon lies on top of the upper plate, is attached to the tank just above the upper plate (where the plate exits the end wall of the tank), and is wrapped around the end and back through the gap between the plates. The lower length of nylon fabric follows a similar route with the lower plate. By pulling the fabric from the tank at speed $2U$, the plates are removed at speed U, with the shear being confined between the plates and the nylon, rather than being transmitted to the fluid. This effectively eliminates the viscous boundary layers. However, in the experiments of Dalziel (1993) and Dalziel *et al.* (1999), the void created by removing this composite barrier was filled asymmetrically by the upper layer descending. This provides an inviscid mechanism for introducing a two-dimensional vortex sheet. Although the resulting motion is very weak compared with those found in the developing R–T flow, it nevertheless seeds a large-scale

Downloaded from http://rsta.royalsocietypublishing.org/ on October 21, 2018

Figure 7. Early three-dimensional development of R–T as the composite barrier (white band near the top of the picture) is withdrawn. (Photograph courtesy of A. G. W. Lawrie, University of Cambridge.)

two-dimensional component that persists throughout each experiment. Figure 7 shows that the developing flow has a clear three-dimensional character growing from high wavenumbers even from the earliest times. But, as seen in figure 8, there is a two-dimensional low-wavenumber component that accelerates a jet down the right-hand wall. It is worth noting that this two-dimensional component associated with the finite volume of the barrier will have been present also in the simple plate experiments of Linden and Redondo, but was masked by the much stronger viscously induced component. Recent work in Cambridge has shown that a significant reduction in the initial perturbation can be achieved by symmetrically filling the void left by the barrier.

The low Atwood numbers (typically 10^{-2}–10^{-3}) used in the SB experiments allowed refractive index matching and major advances in optical diagnostics to be employed, including particle tracking velocimetry, PLIF and pH measurements to directly assess molecular mixing. By characterizing the two-dimensional component of the initial perturbation and feeding this into numerical simulations, Dalziel *et al.* (1999) were able to obtain a level of agreement between simulations and experiments not previously possible. However, obtaining reliable quantitative results required large ensembles of experiments owing to the evolving nature of the flow.

More recently, the Cambridge facility has been used to investigate the effect of an initial tilt on the interface (Holford *et al.* 2003), and the development of R–T in more complex stratifications (Jacobs & Dalziel 2005; Lawrie 2009). Simpler sliding plate experiments have also been undertaken in high-aspect-ratio (essentially one-dimensional) geometries, beginning with Debacq *et al.* (2001).

(*d*) *The water tunnel Rayleigh–Taylor experiment*

Partly in response to the concerns and problems described for the OT and SB experiments, and also a growing need for statistical measurements to validate advanced statistical turbulence models, Andrews developed a water tunnel (WT)

Downloaded from http://rsta.royalsocietypublishing.org/ on October 21, 2018

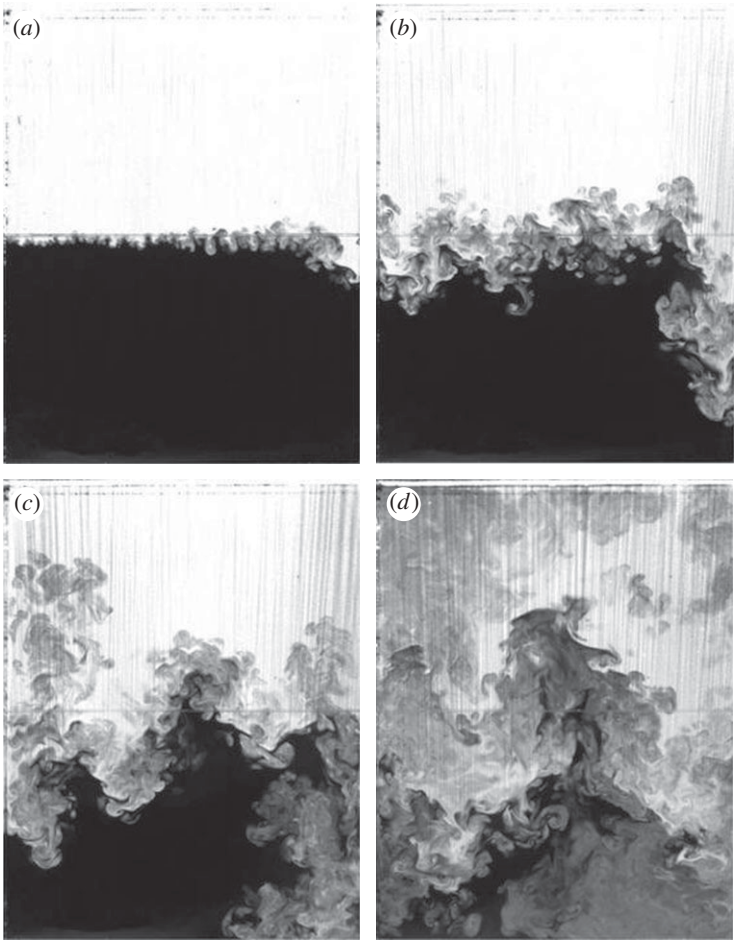

Figure 8. PLIF images of R–T evolution in a composite sliding plate experiment with $A_t = 2 \times 10^{-3}$. Times: (*a*) $t = 0$, the end of barrier removal, (*b*) $t = 5$ s, (*c*) $t = 10$ s and (*d*) $t = 15$ s.

experiment at Texas A&M University. The idea was to generate a statistically steady R–T experiment by way of a WT, as shown in figure 9. As the figure shows, cold water is brought above a splitter plate, and warm water below. Off the end of the splitter plate, the heavy fluid (cold water) sits above light fluid (warm water) and a buoyancy-driven (R–T) mixing layer develops downstream. The temperatures used in this experiment are typically 20°C for the cold fluid, and 25°C for the warm. An equation of state for water by Kukulka (1981) is used to calculate the water densities, and the corresponding Atwood number is 7.4×10^{-4}, a small Atwood number indeed, but still sufficient to see significant mixing, as the photograph shows. The original development of this experiment took place over 1991 and 1992, with extensive tests and checks that included the following (Snider 1994; Snider & Andrews 1994, 1995, 1996):

— Front- and back-wall effects were studied, to ensure that the walls were far enough apart.
— The dye was calibrated using a wedge.

Downloaded from http://rsta.royalsocietypublishing.org/ on October 21, 2018

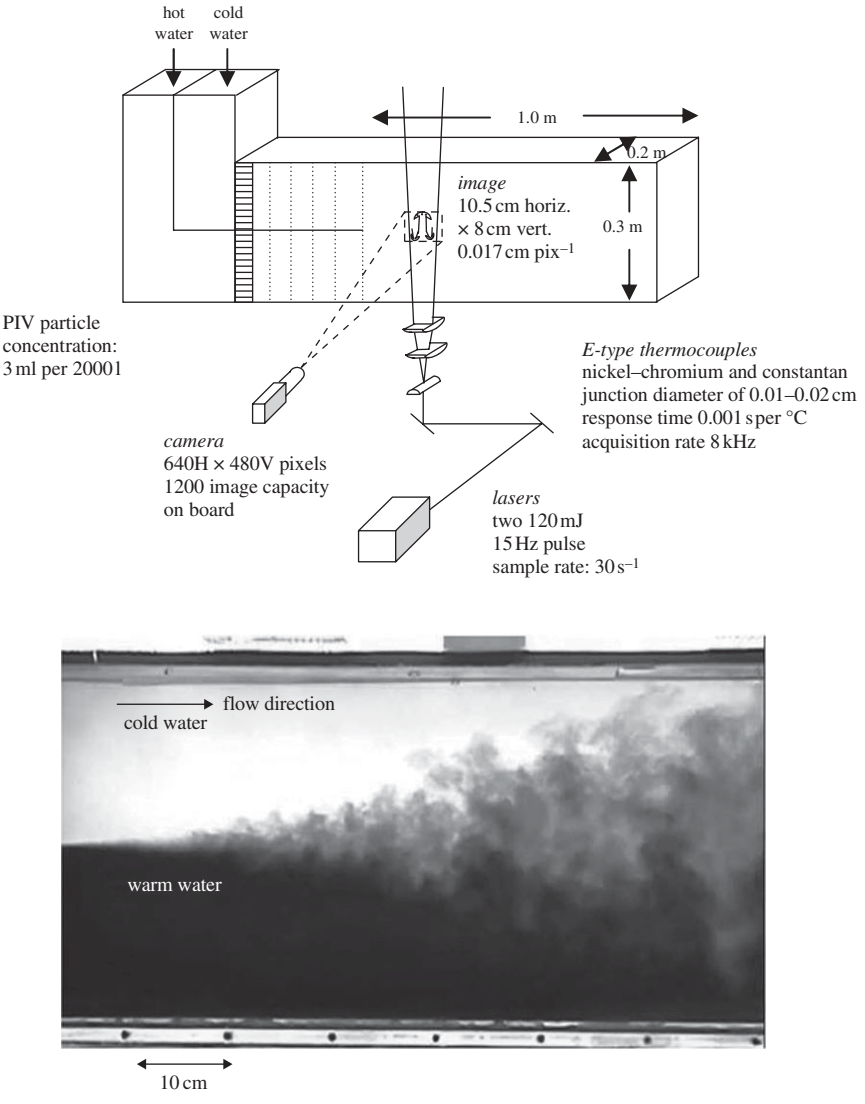

Figure 9. The Texas A&M University SSAA water tunnel R–T experiment.

— Techniques were developed to ensure that the flows advected downstream at the same velocity. Initially, rotameters were used, but they were found to be inaccurate. Thereafter, dye markers were introduced upstream at the same time and place, and were followed. The flow velocity was then adjusted so that the markers stayed in the same relative position.
— Screens were introduced to control the boundary layer thickness at the end of the splitter plate, and along its length.
— It was found that the flows outside the mixing layer were laminar.
— A plate was introduced at the top surface to prevent any asymmetry due to boundary layer development on the bottom of the channel (the boundary layer was at most 0.5 cm thick).

Downloaded from http://rsta.royalsocietypublishing.org/ on October 21, 2018

A water tunnel was chosen, rather than a gas tunnel, because of the inexpensive fluid, ease of creating the density difference (a hot-water tank), availability of flow diagnostics (dye, thermocouples, planar image velocimetry (PIV and later, PLIF), alkali/acid/indicator diagnostics for molecular mixing) and safety. The trade-offs were the small Atwood number and the relatively large volumes of fluid (two 1.9 m^3 tanks were used) limiting the use to miscible fluids.

Over the 15 years of the experimental facility, data collection progressed through a series of refined diagnostics, starting with flow visualization by Snider & Andrews (1994), followed by the spectral measurements of Wilson & Andrews (2002) and culminating in advanced PIV diagnostics used in Ramaprabhu & Andrews (2004). Recent work by Mueschke *et al.* (2009) has used chemical indicators with acid/alkali fluid combinations to obtain direct measurements of molecular mixing. The results suggest that, after an initial (early-time) strong effect of the Schmidt or Prandtl number, the molecular mixing fraction settles to a constant high value of about 0.7 for Reynolds numbers Re_h (defined as $Re_h = 0.35\sqrt{A_t g h^3}/\nu$) greater than 2000, despite the different fluid combinations used, i.e. brine/water with Sc approximately 700, and hot/cold water with Pr approximately 7. Furthermore, a new gas tunnel experiment at Texas A&M University has been developed for high Atwood number R–T studies (Banerjee & Andrews 2006).

3. Conclusions

The past 20 years have seen the remarkable development of effective and useful small Atwood number (less than 0.1) R–T experiments. These experiments have taken advantage of recent developments with diagnostics, and indeed the experiments have prompted at least some of the diagnostic development. The success of the small Atwood number experiments is demonstrated by the extensive datasets that have been collected, and the publications that have resulted (many of which are included in the references presented here). Presently, these datasets are being used to explore the fundamental physics of buoyancy-driven turbulence, and as canonical datasets for turbulence model development and simulation code validation. There is still more research to be done for small Atwood number R–T mixing, which includes two/three-dimensional experiments, coupled experiments involving shear and buoyancy, the effects of initial conditions, higher Reynolds number, high Schmidt number effects (immiscible fluids) and cross-coupling with chemistry/heat release.

Returning to the Youngs (1984) description of the development of R–T, the experiments described here have been effective in addressing the growth during the third step, and to some extent the transition within the second step, but the early-time linear growth has remained elusive and for a long time was considered unimportant. Increasing the viscosity of the working fluid is one route for providing more information on this early-time behaviour, but the development of boundary layers hampers the use of overturning or WT experiments, and the slower growth rates would require longer travels for RR experiments. It is unclear whether the void produced by the removal of the SB would contaminate very low Reynolds number experiments, as such

Downloaded from http://rsta.royalsocietypublishing.org/ on October 21, 2018

experiments have not historically been a research priority, but perhaps this should be addressed as part of the effort to better understand the role of initial conditions.

We noted some difficulties with high Atwood number (more than 0.1) experiments, but we confidently expect our concerns to be addressed in the near future, and that datasets similar to the small Atwood number ones discussed here will become available. Indeed, progress towards this goal is already being made. Although most earlier high Atwood number R–T experiments were with immiscible fluids, considerable effort now appears to be focused on miscible systems. In addition to the gas tunnel results noted previously (Banerjee & Andrews 2006), preliminary experiments using a variation on the RR (Roberts & Jacobs 2008), and high-pressure gas systems (Kucherenko *et al.* 2003), along with novel approaches such as magnetorheological fluids (White *et al.* 2004), are showing considerable promise, although further progress on the associated diagnostics is necessary to provide the much-needed measurements in this miscible regime.

The water tunnel experiments referred to in this paper were performed in the Stockpile Stewardship Academic Alliances (SSAA) laboratory of Andrews at Texas A&M University by Dale Snider, Peter Wilson, Praveen Ramaprabhu, Arindam Banerjee, Wayne Kraft and Nicholas Mueschke, with the support of the US Department of Energy under contracts DE-FG03-99DP00276/A000, DE-FG03-02NA00060 and DE-FG52-06NA26154. Dalziel's sliding barrier experiments were supported by AWE through an extended series of contracts with the assistance of Paul Linden, José Redondo, Joanne Holford, David Leppinen and Andrew Lawrie.

References

Abarzhi, S. I., Nishihara, K. & Glimm, J. 2003 Rayleigh–Taylor and Richtmyer–Meshkov instabilities for fluids with a finite density ratio. *Phys. Lett. A* **317**, 470. (doi:10.1016/j.physleta.2003.09.013)

Abarzhi, S. I., Gauthier, S. & Rosner, R. 2008 Turbulent mixing and beyond. *Physica Scr.* **T132**, 011001. (doi:10.1088/0031-8949/2008/T132/011001)

Andrews, M. J. 1986 Turbulent mixing by Rayleigh–Taylor instability. PhD dissertation, London University, UK.

Andrews, M. J. & Spalding, D. B. 1990 A simple experiment to investigate two-dimensional mixing by Rayleigh–Taylor instability. *Phys. Fluids A* **2**, 922–927. (doi:10.1063/1.857652)

Banerjee, A. & Andrews, M. J. 2006 Statistically steady measurements of Rayleigh–Taylor mixing in a gas channel. *Phys. Fluids* **18**, 035107. (doi:10.1063/1.2185687)

Burrows, K. D., Smeeton, V. S. & Youngs, D. L. 1984 Experimental investigation of turbulent mixing by Rayleigh–Taylor instability, II. AWRE Report no. 022/84.

Dalziel, S. B. 1993 Rayleigh–Taylor instability: experiments with image analysis. *Dyn. Atmos. Oceans* **20**, 127–153. (doi:10.1016/0377-0265(93)90051-8)

Dalziel, S. B., Linden, P. F. & Youngs, D. L. 1999 Self-similarity and internal structure of turbulence induced by Rayleigh–Taylor instability. *J. Fluid Mech.* **399**, 1–48. (doi:10.1017/S002211209900614X)

Dalziel, S. B., Patterson, M. D., Caulfield, C. P. & Coomaraswamy, I. A. 2008 Mixing efficiency in high-aspect-ratio Rayleigh–Taylor experiments. *Phys. Fluids* **20**, 065106. (doi:10.1063/1.2936311).

Debacq, M., Fanguet, V., Hulin, J. P. & Salin, D. 2001 Self-similar concentration profiles in buoyant mixing of miscible fluids in a vertical tube. *Phys. Fluids* **13**, 3097–3100. (doi:10.1063/1.1405442)

Dimonte, G. (ed.) 2008 *Proc. 11th Int. Workshop on the Physics of Compressible Turbulent Mixing, Santa Fe, NM.* Los Alamos Report no. LA-UR-08-4321. (http://iwpctm.org/proceedings/)

Downloaded from http://rsta.royalsocietypublishing.org/ on October 21, 2018

Dimonte, G. & Schneider, M. 1996 Turbulent Rayleigh–Taylor instability experiments with variable acceleration. *Phys. Rev. E* **54**, 3740–3743. (doi:10.1103/PhysRevE.54.3740)

Drazin, P. G. & Reid, W. H. 1981 *Hydrodynamic stability.* Cambridge, UK: Cambridge University Press.

Emmons, H. W., Chang, C. T. & Watson, B. C. 1960 Taylor instability of finite surface waves. *J. Fluid Mech.* **7**, 177–193. (doi:10.1017/S0022112060001420)

Goncharov, V. N. 2002 Analytical model of nonlinear, single-mode, classical Rayleigh–Taylor instability at arbitrary Atwood numbers. *Phys. Rev. Lett.* **88**, 134 502. (doi:10.1103/PhysRevLett.88.134502)

Holford, J. M., Dalziel, S. B. & Youngs, D. L. 2003 Rayleigh–Taylor instability at a tilted interface in laboratory experiments and numerical simulations. *Lasers Part. Beams* **21**, 491–423. (doi:10.1017/S0263034603213203)

Jacobs, J. & Dalziel, S. B. 2005 Rayleigh–Taylor instability in complex stratifications. *J. Fluid Mech.* **542**, 251–279. (doi:10.1017/S0022112005006336)

Kraft, W., Andrews, M. J., Ramaprabhu, P. & Snider, D. 2005 Visualization of the Rayleigh–Taylor instability. *J. Flow Visualization* **12**, 363–375. (doi:10.1615/JFlowVisImageProc.v12.i4.30)

Kucherenko, Yu. A., Balabin, S. I., Ardashova, R. I., Kozelkov, O. E., Dulov, A. V. & Romanov, I. A. 2003 Experimental study of the influence of the stabilizing properties of transitional layers on the turbulent mixing evolution. *Laser Part. Beams* **21**, 369–373. (doi:10.1017/S0263034603213124)

Kukulka, D. J. 1981 Thermodynamic and transport properties of pure and saline water. MS dissertation, State University of New York at Buffalo, USA.

Lawrie, A. G. W. 2009 Rayleigh–Taylor mixing: confinement by stratification and geometry. PhD thesis, DAMTP, University of Cambridge, UK.

Layzer, D. 1955 On the instability of superposed fluids in a gravitational field. *Astrophys. J.* **122**, 1–12. (doi:10.1086/146048)

LeLevier, R., Lasher, G. J. & Bjorklund, F. 1955 Effect of a density gradient on Taylor instability. UCRL Report no. 4459.

Linden, P. F. & Redondo, J. M. 1991 Molecular mixing in Rayleigh–Taylor instability. Part I: Global mixing. *Phys. Fluids A* **3**, 269–1277. (doi:10.1063/1.858055)

Linden, P. F., Redondo, J. M. & Youngs, D. I. 1994 Molecular mixing in Rayleigh–Taylor instability. *J. Fluid Mech.* **265**, 97–124. (doi:10.1017/S0022112094000777)

Mueschke, N. J., Andrews, M. J. & Schilling, O. 2006 Experimental characterization of initial conditions and spatio-temporal evolution of a small Atwood number Rayleigh–Taylor mixing layer. *J. Fluid Mech.* **567**, 27–63.

Mueschke, N. J., Schilling, O., Youngs, D. L. & Andrews, M. J. 2009 Measurements of molecular mixing in a high Schmidt number Rayleigh–Taylor mixing layer. *J. Fluid Mech.* **632**, 17–48. (doi:10.1017/S0022112009006132)

Ramaprabhu, P. & Andrews, M. J. 2004 Experimental investigation of Rayleigh–Taylor mixing at small Atwood numbers. *J. Fluid Mech.* **502**, 233–271. (doi:10.1017/S0022112003007419)

Ramaprabhu, P. & Dimonte, G. 2005 Single-mode dynamics of the Rayleigh–Taylor instability at any density ratio. *Phys. Rev. E* **71**, 036314. (doi:10.1103/PhysRevE.71.036314)

Ramaprabhu, P., Dimonte, G., Young, Y.-N., Calder, A. C. & Fryxell, B. 2006 Limits of the potential flow approach to the single-mode Rayleigh–Taylor problem. *Phys. Rev. E* **74**, 066308. (doi:10.1103/PhysRevE.74.066308)

Read, K. I. 1984 Experimental investigation of turbulent mixing by Rayleigh–Taylor instability. *Physica D* **12**, 45–58. (doi:10.1016/0167-2789(84)90513-X)

Read, K. I. & Youngs, D. L. 1983 Experimental investigation of turbulent mixing by Rayleigh–Taylor instability. AWRE Report no. 011/83.

Ristorcelli, J. R. & Clark, T. T. 2004 Rayleigh–Taylor turbulence: self-similar analysis and direct numerical simulations. *J. Fluid Mech.* **507**, 213–253. (doi:10.1017/S0022112004008286)

Roberts, M. & Jacobs, J. 2008 Experiments on the Rayleigh–Taylor instability of a large Atwood number, miscible fluid combination. In *Proc. 11th Int. Workshop on the Physics of Compressible Turbulent Mixing, Santa Fe, NM* (ed. G. Dimonte). Los Alamos Report no. LA-UR-08-4321. (http://iwpctm.org/proceedings/)

Downloaded from http://rsta.royalsocietypublishing.org/ on October 21, 2018

Smeeton, V. S. & Youngs, D. L. 1987 Experimental investigation of turbulent mixing by Rayleigh–Taylor Instability, III. AWRE Report no. 035/87.

Snider, D. M. 1994 Rayleigh–Taylor and shear driven mixing. PhD dissertation, Texas A&M University, USA.

Snider, D. M. & Andrews, M. J. 1994 Rayleigh–Taylor and shear driven mixing with an unstable thermal stratification. *Phys. Fluids* **6**, 3324–3334. (doi:10.1063/1.868065)

Snider, D. M. & Andrews, M. J. 1995 An inexpensive method for quantitative data collection from photographic prints. *Meas. Sci. Technol.* **6**, 502–506. (doi:10.1088/0957-0233/6/5/011)

Snider, D. M. & Andrews, M. J. 1996 The structure of shear driven mixing with an unstable thermal stratification. *ASME J. Fluids Eng.* **118**, 55–60. (doi:10.1115/1.2817511)

Turner, J. S. 1973 *Buoyancy effects in fluids*. Cambridge, UK: Cambridge University Press.

Voropayev, S. I., Afanasyev, Y. D. & van Heijst, G. J. F. 1993 Experiments on the evolution of gravitational instability of an overturned, initially stably stratified fluid. *Phys. Fluids A* **5**, 2461–2466. (doi:10.1063/1.858759)

White, J., Selig, C., Oakley, J., Anderson, M. & Bonazza, R. 2004 The Rayleigh–Taylor instability at a water/magnetorheological fluid interface. In *Proc. 9th Int. Workshop on the Physics of Compressible Turbulent Mixing, Cambridge, UK* (ed. S. B. Dalziel). (http://iwpctm.org/proceedings/)

Wilson, P. N. & Andrews, M. J. 2002 Spectral measurements of Rayleigh–Taylor mixing at low Atwood number. *Phys. Fluids A* **14**, 938–945. (doi:10.1063/1.1445418)

Youngs, D. L. 1984 Numerical simulation of turbulent mixing by Rayleigh–Taylor instability. *Physica D* **12**, 32–44. (doi:10.1016/0167-2789(84)90512-8)